Electrochemical and Spectroscopic Studies on Copper(II) Complexes of Macrocyclic Ligands as Models for Square-Pyramidal Metal Active Sites of Copper(II) Complexes of Bleomycin and Glutathione

KIYONORI MIYOSHI

Department of Metallurgical Engineering, Niihama Technical College, Niihama 792, Japan

HISASHI TANAKA

Faculty of Pharmaceutical Science, Kyoto University, Kyoto 606, Japan

EIICHI KIMURA

Institute of Pharmaceutical Science, Hiroshima University School of Medicine, Hiroshima 734, Japan

SEI TSUBOYAMA

The Institute of Physical and Chemical Research, Wako-shi, Saitama 351, Japan

SHIZUO MURATA, HIROAKI SHIMIZU and KAZUHIKO ISHIZU

Department of Chemistry, Faculty of Science, Ehime University, Matsuyama, Ehime 790, Japan

Received June 16, 1982

The properties of Cu(II) complexes of saturated macrocyclic ligands with square-pyramidal array were examined by cyclic voltammetry, electron spin resonance, visible absorption and magnetic circular dichroism spectroscopy. All ligands used with N_4, N_5, N_6, N_4S and N_4O donor sets coordinated to Cu(II) to form a chromophore by the same donor set N_4 at the equatorial plane. The values of λ_{max} vs. $E_{1/2}$ and $g_{\parallel}$ vs. $1/E_{1/2}$ showed excellent linear correlations; however, the complexes containing O and S ligation exhibited marked deviations from the correlations. Of special interest is the fact that the physicochemical data of the $15N_5$–Cu(II) complex are substantially similar to those from the naturally occurring bleomycin–Cu(II) complex, in which the axially coordinated primary amino group plays a significant role for antitumor activity. With replacement of the axial N donor with the O and S donor, a marked positive shift was recognized in the $E_{1/2}$ values in the order of $S > O > N$. A positive shift of $E_{1/2}$ value, which is a feature of the apical S-donor in the square-pyramidal $15N_4S$–Cu(II) complex, was consistently seen for the glutathione–Cu(II) complex.

Introduction

Interest in complexes of fully saturated macrocyclic ligands is growing as potential models of naturally occurring and biologically important complexes such as metallo porphins, ionophores, metal carrier proteins, metallo enzymes or antibiotic peptides. There are distinctive advantages of macrocyclic ligands as these models are easily designed to mimic the metal active site in biological systems [1].

The recent findings in our laboratory that a naturally occurring anticancer agent, bleomycin (BLM)–Cu(II) complex [2], and violet glutathione–Cu(II) complex [3] have square-pyramidal configuration at Cu(II) chromophore, led us to investigate the physicochemical properties of active centers by using a series of simple saturated macrocyclic ligands. It is proposed that both the fifth axial N donor and rigid square-pyramidal coordination for BLM are essential for effective molecular oxygen binding and efficient oxygen reduction [4]. In addition, X-ray analysis of the violet glutathione–Cu(II) complex showed the unique axial S ligation by cysteinyl residue [3].

In this paper, therefore, we focused on the properties of the square-pyramidal coordination geometry and its axial ligation donor for Cu(II) complex, since these are suggested to be the active center in type 2 copper protein [5, 6]. The possibility of N axial ligation, which has cloudily often been detected in the ESR of Cu(II) complex, is well documented by the ESR of corresponding Ni(III) complexes [7–10]. The present notions by the combination of electro-

0020-1693/83/0000-0000/$03.00

chemical and spectroscopic features characterize the Cu(II) active center with square-pyramidal configuration and respective fifth axial N, S and O donors.

Experimental

The materials used (Scheme 1) were prepared according to the methods already reported [11–13]

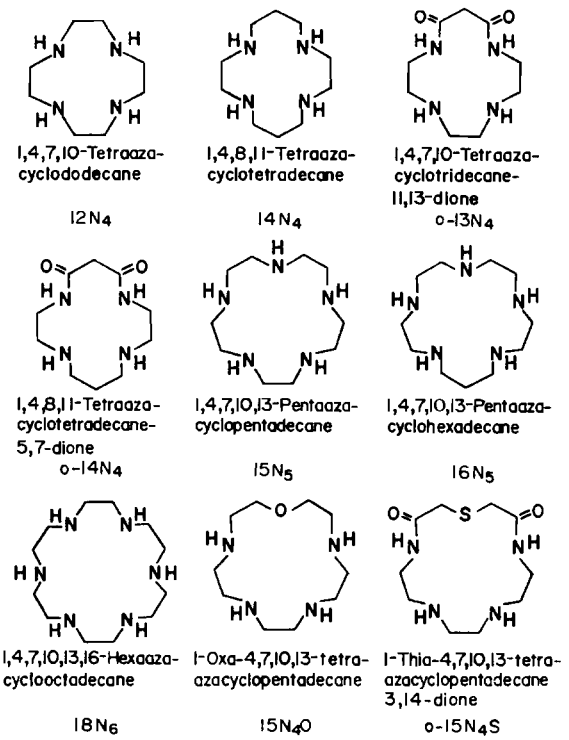

Scheme 1. Saturated macrocyclic ligands used for the present study.

and checked with elemental analysis and NMR spectra. The solution of 1:1 Cu(II)–ligand (L) complexes were prepared by mixing macrocyclic ligands and $CuCl_2$ in borate buffer solution (pH 9), where all the complexes are present as CuL^{2+}, except those containing amide group as $CuH_{-2}L^0$ [11, 12, 14]. On the other hand, the 1:1 relatively stable Ni(III) complexes of some macrocyclic ligands were obtained by chemical oxidation of the corresponding Ni(II) complexes with $Na_2S_2O_8$ in aqueous 50 m*M* acetate buffer solution [15]. The Ni(III) complex of BLM kindly supplied by Nippon Kayaku Co. Ltd, was also prepared in a similar manner. The solution of Ni(III) complex was immediately frozen in liquid nitrogen and ESR measurements were carried out.

Visible absorption spectra of 1:1 Cu(II)–L complexes were recorded by a Hitachi recording spectrometer Model 200-20. Magnetic circular dichroism (MCD) spectra were taken with a Jasco J-20 spectropolarimeter equipped with a 10.4 KG electromagnet. ESR spectra were obtained by a JES-ME-3X spectrometer (100 KHz magnetic field modulation) both at room temperature and at 77 K. The $g_\perp$ and $A_\perp$ values were obtained from the approximated tensor average, $g_0 = (g_\parallel + 2g_\perp)/3$ and $A_0 = (A_\parallel + 2A_\perp)/3$. The magnetic field was calibrated by the splitting of Mn(II) in MgO (ΔH_{3-4} = 86.9 G) and g values were standardized by the use of Li–TCNQ (g = 2.0026) as a reference.

Cyclic voltammograms were obtained by a Yanagimoto P-1000H instrument at 25 °C in a mixture of the solution of 1/15 *M* Na_2HPO_4 and 0.1 *M* $NaClO_4$. Cyclic voltammetry was performed with a three-electrode system containing a hanging mercury drop working electrode, a platinum counter electrode, and a saturated calomel reference electrode. Cyclic voltammograms were recorded at a scan rate of 100 mV s^{-1}. Since the qualitative aspects of the electrochemistry of Cu(II)–L depend on the solvent system and the electrode used [16, 17], we carried out the Cu(II)/Cu(I) potential measurements carefully. A platinum working electrode was employed to check the potential peaks. The redox potential $E_{1/2}$ values were determined as the midpoint between the peak potentials, $E_{1/2} = \frac{1}{2}(E_{pc} + E_{pa})$. The determination of the redox potential was checked also by simultaneous polarographic measurement.

Results and Discussion

Visible Absorption Spectra

The visible absorption maxima λ_{max} for Cu(II) complexes of macrocyclic ligands shift to shorter wavelengths in the order o-$14N_4$ > $14N_4$ > o-$13N_4$ > $16N_5$ > o-$15N_4S$ > $15N_4O$ = $15N_5$ > $12N_4$ > $18N_6$, reflecting a certain serial change of the coordination geometry in each metal site. The large red shifts of λ_{max} seen for Cu(II) complexes of 14-membered macrocyclic ligands mean that the strong equatorial ligand field is considered in square-planar basal plane of these Cu(II) chromophores. For the dioxo macrocyclic ligands, the steric requirement leaves only a choice of Cu–N (imide) bonds for full tetradentate coordination. The ability of the N^- (peptide) to act as a strong ligand field donor is documented; it is high in the spectrochemical series, causing λ_{max} to shift to shorter wavelengths than does the N (amino) group.

On the other hand, the opposite red shift and intensity enhancement of the absorption band seen for $12N_4$–Cu(II) complex with smallest ring size is attributed to the distortion from the square-planar to square-pyramidal stereochemistry, apparently caused by the steric constraint [18–20]. For this and the ESR result, Styka *et al.* took the $12N_4$–Cu(II) complex as a model for type 2 copper protein [11].

TABLE I. Electronic and Magnetic Circular Dichroism Spectral Data for Cu(II) Complexes of Saturated Macrocyclic Ligands.

Ligand	λ_{max}, cm^{-1} (ϵ)		MCD Extrema, cm^{-1} ($\Delta\epsilon$/10 kG)		
$12N_4$	16700(220)	–	–	18180(–0.162)	14380(+0.022)
$14N_4$	19500(100)	–	–	20960(–0.064)	17760(+0.023)
o-$13N_4$	19200(100)	–	–	–	–
o-$14N_4$	19700(90)	–	–	21050(–0.050)	18010(+0.026)
$15N_5$	17000(220)	12120(75)	–	18110(–0.149)	14810(+0.008)
$16N_5$	17600(160)	12420(70)	–	–	–
$18N_6$	14300(140)	–	–	15100(–0.10)	–
$15N_4O$	17000(145)	–	–	19120(–0.069)	13420(+0.005)
o-$15N_4S$	17090(125)	14080(90)	25000(+0.005)	19150(–0.077)	13240(+0.011)

TABLE II. Electronic, CD and ESR Spectral Data for Cu(II) Complexes of Bleomycin (BLM), Depyruvamide (dep)-BLM, P-3A and Glutathione.

Ligand	λ_{max} cm^{-1}	CD Extrema, cm^{-1}			$g_\parallel$	$g_\perp$ (g_x/g_y)	$A_\parallel$ cm^{-1} $\times 10^{-4}$	$E_{1/2}$ V, *vs.* SCE
BLM [2]	16800	–	18010	15030	2.211	2.055	178	–0.568
dep-BLM [23]	17800	–	19800	16940	2.174	2.055	193	–0.577
P-3A [23]	16000	–	17240	14280	2.214	2.133 2.078	173	–0.377
GSH [24]	16260	25970	16520	12980	2.258	2.059	174	–0.166

Cu(II) complexes with 15 ring members, $15N_5$, $15N_4O$ and o-$15N_4S$ revealed the extra absorption peak at *ca.* 13000 cm^{-1} further red-shifted from the frequency of the major d–d absorption band. This extra d–d absorption of Cu(II) complex is indicative of axial interaction in a five coordination system [21]. Thus, the five coordinated square-pyramidal structure can be proposed based on the observation of two characteristic bands observed in both visible and near infrared region as shown in Table I [6, 21]. The o-$15N_4S$–Cu(II) complex has two absorption bands, one of which is observed at 17090 cm^{-1}, being close to that of S-methyl glutathione–Cu(II) complex [22]. The MCD extremum at 25000 cm^{-1} for the o-$15N_4S$-Cu(II) complex is assigned to the S → Cu(II) charge transfer transition, which reveals the Cu–S binding on the apex [3]. In Table II, we give the electronic, CD, ESR spectral and redox potential data characterized to the Cu(II) complexes of BLM, its related biosynthetic intermediate [23] and glutathione (green) [24]. It is interesting to note that the observed visible absorption maximum and the CD extrema for the BLM–Cu(II) complex with N_5 donors are very much like the bands of $15N_5$–Cu(II) complex. In contrast, those of the depyruvamide (dep) BLM–Cu(II) complex with N_4 donors obtained by removal of the apical α-amino group, are shifted to shorter wavelengths to a large extent. The facts of a notable blue shift in the d–d band ($d_{xz,yz} \rightarrow d_{x^2-y^2}$ and $d_{xy} \rightarrow d_{x^2-y^2}$) as characterized to Cu(II) complexes of macrocyclic polyamine and dep-BLM having N_4 donors mean that the in-plane σ-antibonding will rise in energy as the ligand coplanarity strengthens, while the π-antibonding d_{xz} and d_{yz} orbitals will decrease in energy [25]. Thus, the blue shift in the λ_{max} observed for the dep-BLM–Cu(II) complex means a weakened axial interaction and an increase in the in-plane field strength as demonstrated for macrocyclic polyamine ($14N_4$ and o-$14N_4$) ligands by reducing the number of N donors from five ($15N_5$ and $16N_5$) to four. In contrast, a marked shift in λ_{max} to 14300 cm^{-1} characteristic of the $18N_6$–Cu(II) complex is reminiscent of an octahedrally distorted coordination environment in the Cu(II) chromophore.

Axial Ligations for Cu(II) Complex by ESR of Corresponding Ni(III) Complex

The positive identification of the equatorial N_4 donor set coordinating to the Cu(II) atom can be obtained by detection of the ligand N superhyper-

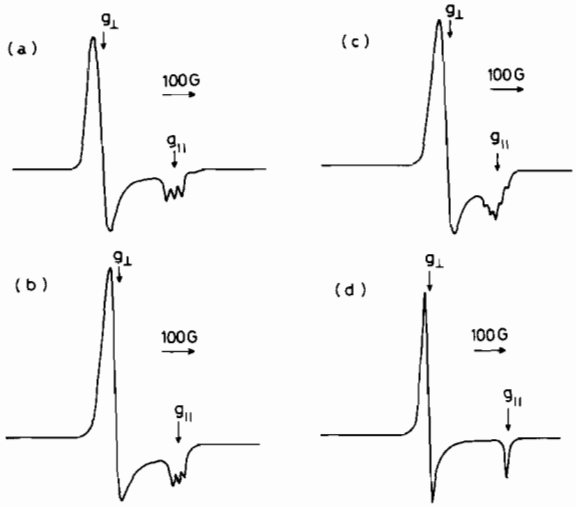

Fig. 1. ESR spectra for Ni(III) complexes of (a) BLM, (b) $15N_5$, (c) $18N_6$ and (d) $15N_4O$ at 77 K.

fine splitting. For apical binding, however, ESR detection of the axial N is usually insensitive for Cu(II) complexes. In these cases, Ni(III) complexes analogous to Cu(II) complexes with $3d_{z^2}$ ground state are employed to examine the fact of apical coordination due to an N donor [7–10]. Although the trivalent state of Ni has been considered to be a relatively rare oxidation state, some recent studies suggest that numerical macrocyclic ligands give a long-lived Ni(III) complex stabilized by macrocyclic effect [7, 8]. The ESR spectra of low spin Ni(III) complexes were successfully observed for BLM, $15N_5$, $18N_6$ and $15N_4O$ ligands as can be seen in Fig. 1. The ESR line shape recorded for the $15N_5$–Ni(III) complex is typical of $3d_{z^2}$ ground state with $3d^7$ low spin (S = ½) configuration, in which one axial N ligation is visualized with extra three line superhyperfine splitting due to the mononuclear N atom (I = 1) [7–10]. The superhyperfine splitting with intensity ratio 1:2:3:2:1 in $g_{\parallel}$ component for $18N_6$–Ni(III) complex shows that two equivalent N atoms in the axial position coordinate to Cu(II). All the coordination sites of $18N_6$ hold the octahedral coordination geometry. In contrast, no extrahyperfine splitting is detected for $15N_4O$–Ni(III) complex, in which the apical coordination of O donor would be probable. Of particular interest is the fact that BLM also generates a relatively stable Ni(III) low spin complex and the ESR parameters are like those observed for the pentadentate $15N_5$–Ni(III) complex, as shown in Table III. The evidence is consistent with the fact that an apical α-amino N ligation is probable, as already proposed for the BLM–Cu(II) complex [2, 26].

Sixth apical ligation due to the mannose carbamoyl group has been proposed for the BLM–Cu(II) complex [2, 26]. In the BLM–Ni(III) complex, however, the N superhyperfine splitting due to the sixth carbamoyl group was not observed. This means that the mannose carbamoyl group coordinates with carbonyl group but not with amide N atom at the sixth position, thus the lesser extent of spin density on the carbamoyl N can hardly be detected in the ESR spectrum.

TABLE III. ESR Parameters for Ni(III) Complexes of Bleomycin (BLM) and Saturated Macrocyclic Ligands.

Ligand	$g_{\parallel}$	$g_\perp$	$A_{\parallel}$ (G)
BLM	2.021	2.164	21.5
$15N_5$	2.023	2.149	17.7
$18N_6$	2.024	2.123	17.6
$15N_4O$	2.026	2.187	–

ESR of Cu(II) Complexes

The Cu(II) ESR spectra measured for macrocyclic ligands, BLM and glutathione are typical of tetragonal Cu(II) complex with $d_{x^2-y^2}$ ground state doublet [27]. The observed tendencies for $A_{\parallel}$ to increase and $g_{\parallel}$ to decrease have been taken as parameters to measure the strength of in-plane ligand fields under the tetragonal basal square arrangement of Cu(II) complexes [28]. In addition, the bonding natures between the metal and the equatorial ligand N atoms have been discussed in detail, based on the ligand N superhyperfine splitting in terms of the molecular orbital involving Cu(II) $3d^9$ and the ligand N atomic orbitals. From inspection of ESR parameters of Cu(II) complex listed in Table IV, a feature of coordination geometry in each complex can be extracted.

The Cu(II) complexes of $14N_4$, o-$14N_4$ and o-$13N_4$ as characterized by relatively larger $A_{\parallel}$ (*ca.* 200 × 10^{-4} cm^{-1}) values and lower $g_{\parallel}$ (*ca.* 2.18) values are likely to take square-planar geometry. In fact, the spin densities on the Cu(II) $3d_{x^2-y^2}$, $\alpha^2 = 0.80$ estimated from the ligand N superhyperfine splitting (A_N), are consistent with those of the Cu(II) complex with a square-planar geometry [28]. The opposite trend of $g_{\parallel}$ and $A_{\parallel}$ values is seen for $12N_4$–Cu(II) complex with the cavity size, which is too small to accommodate Cu(II) ions. The larger $g_{\parallel}$ and smaller $A_{\parallel}$ are associated with an off-planar distortion, probably into the pyramidal geometry.

It has been known that the hyperfine tensor components $A_{\parallel}$ of some Cu(II) complexes decrease upon axial coordination due to a reduction in the d-orbital spin density and/or admixing of 4s character into the antibonding orbital of singly occupied $3d^9$ system [29, 30]. Reduction (*ca.* 20 × 10^{-4}

TABLE IV. ESR Parameters and Redox Potentials for Cu(II) Complexes of Saturated Macrocyclic Ligands.

Ligand	$g_\parallel$	$g_\perp$	$A_\parallel$	$A_\perp$	$E_{1/2}$ V, *vs.* SCE
			$\times 10^{-4}$ cm^{-1}		
$12N_4$	2.198	2.057	184.2	24.1	−0.642
$14N_4$	2.186	2.049	205.0	38.7	−0.729
o-$13N_4$	2.171	2.046	202.8	28.5	−0.742[a]
o-$14N_4$	2.176	2.049	207.4	37.1	−0.848[a]
$15N_5$	2.203	2.054	182.6	25.7	−0.570
$16N_5$	2.200	2.057	187.8	24.9	−0.562
$18N_6$	2.241	2.063	159.1	22.1	−0.440
$15N_4O$	2.201	2.049	192.2	32.9	−0.406
o-$15N_4S$	2.204	2.057	182.3	28.9	−0.186

[a]The value is shown by E_{pc} due to irreversible cyclic voltammogram.

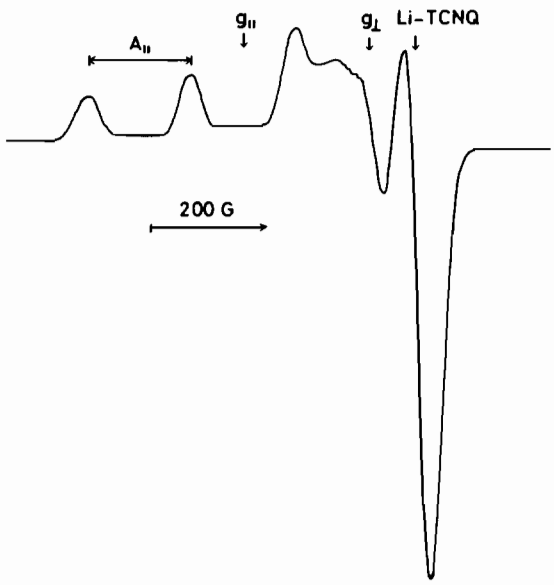

Fig. 2. ESR spectrum of o-$15N_4S$–Cu(II) complex at 77 K.

cm^{-1}) in $A_\parallel$ values seen for $15N_5$ and $16N_5$ complexes from the corresponding values of the square-planar $14N_4$, o-$14N_4$ and o-$13N_4$ complexes indicates the effect due to the axial coordination of the fifth N atom in addition to the effect of off-planar distortion occurring in Cu(II) square-planar basal plane.

The o-$15N_4S$–Cu(II) complex has similar ESR parameters to those of $15N_5$–Cu(II) complex. Combining both the major d–d absorption band to 5 nm blue shift and ESR spectra with the nine lines of N superhyperfine splitting, a contribution of $3d_{x^2-y^2}$ orbital for the o-$15N_4S$ complex is probably higher than those of macrocyclic pentaamine–Cu(II) complexes. Thus, the stronger effect of the axial S donor as compared with N donor is indicative of a slightly strong perturbation to Cu(II) chromophore.

Of special interest is that the $A_\parallel$ value of o-$15N_4S$ complex is close to that of the violet glutathione–Cu(II) complex [3]. As seen in Fig. 2, the coordinated Cu(II) complex exhibits the nonequivalence in the equatorial g-anisotropy. This may be attributed to a marked deviation of the axial Cu–S bond from the unique axis of the tetragonal square basal plane, as has been demonstrated for violet glutathione–Cu(II) complex with a distorted square-pyramidal structure [3].

The $18N_6$–Cu(II) complex has unique structural features, as revealed by an anomalously small $A_\parallel$ value with relatively high $g_\parallel$ value. The extremely small $A_\parallel$ value and large $g_\parallel$ value in this case can be explained in terms of the constrained octahedral environment, which is a rare coordination configuration among multidentate ligand–Cu(II) complexes [31, 32].

We have already recognized that the ESR parameters of the $15N_5$–Ni(III) complex is fairly close to those of Ni(III) complex of BLM. It is thus interesting to see here how the similarity of the ESR parameters can be held in the case of Cu(II) complexes. In Tables II and IV, a striking similarity of the ESR parameters can be seen between $15N_5$–Cu(II) complex and BLM–Cu(II) complex, where the N^π and the deprotonated amide N of β-hydroxyhistidine, the N-1 of the 4-aminopyrimidine ring and the secondary amino group occupy the square basal position N_4 with the primary amino group at the square-pyramidal position, and the O-carbamoyl group at the sixth coordination site [2, 26]. In fact, BLM coordinates to Cu(II) ion as the pentadentate N ligand, thus taking Cu–N_5 square-pyramidal structure. The effect of the apical coordination is evident in comparison with the parameters of dep-BLM–Cu(II) complex and those of BLM–Cu(II) complex, where $A_\parallel$ values become larger than that of BLM–Cu(II) complex and $g_\parallel$ value is smaller. A similarity is also recognized between the ESR parameters of the dep-BLM–Cu(II) and 14-membered N_4–Cu(II) complexes. This implies that the Cu(II) chromophore of dep-BLM involving the secondary amino N, pyrimidine (N-1) ring N, deprotonated peptide and N^π of β-hydroxyhystidine is likely to be present in a square-planar geometry.

Redox Potentials

Although coordination structures of Cu(II) sites have often been discussed in detail on the ESR parameters, perturbations on the g- and A-tensors resulting from axial ligation are more or less insensitive for $3d_{x^2-y^2}$ ground state. In order to characterize the difference in the coordination environment among Cu(II) complexes more severely, the redox poten-

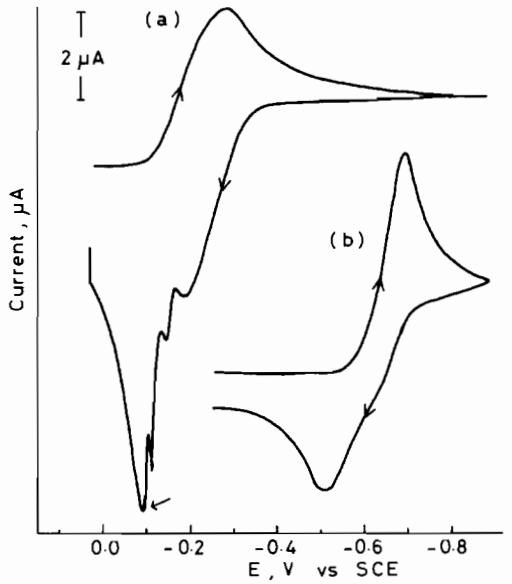

Fig. 3. Cyclic voltammograms for the Cu(II) complexes of (a) o-$15N_4S$ and (b) $15N_5$ in aqueous solution at a hanging drop mercury electrode. An arrow indicates the E_{pa} of Cu(II)/Cu(I) couple.

tials ($E_{1/2}$) of the Cu(II) complexes were measured.

All $E_{1/2}$ values determined by cyclic voltammograms (CV) already listed in Table IV, are given in terms of standard electrode potential *vs.* SCE. One of the typical CV figures measured for the Cu(II)/Cu(I) coupled reaction in the $15N_5$–Cu(II) complex is shown in Fig. 3. In the case of the o-$15N_4$-S–Cu(II) complex (Fig. 3), true Cu(II)/Cu(I) E_{pa} peaks among four E_{pa} values are determined preferentially by using a platinum working electrode, and thus, the other three peaks are considered as electrochemical reactions on the basis of specific affinities between Hg and S atoms of the ligand. The CV figures display the typical patterns of reversible or quasi-reversible one electron redox-reaction for the present macrocyclic ligand–Cu(II) complexes except o-$13N_4$ and o-$14N_4$ complexes. In the present potential range, the CV peaks defined to the ligand reduction or oxidation have not been detected [33, 34].

As shown in Table IV, $E_{1/2}$ values for the macrocyclic polyamine–Cu(II) complexes are in the range −0.85 to −0.44 V. Among the complexes with reversible Cu(II)/Cu(I) couple, the square-planar $14N_4$–Cu(II) complex gives the most negative value. The most negative values reported for Cu(II) complexes of o-$14N_4$ and o-$13N_4$ reflect the irreversible redox reaction, owing to its strengthened square-planar configuration, as seen in visible absorption and ESR spectra. The square-pyramidal Cu(II) complexes of $12N_4$, $15N_5$ and $16N_5$ show the slightly positive $E_{1/2}$ values in comparison with square-planar com-

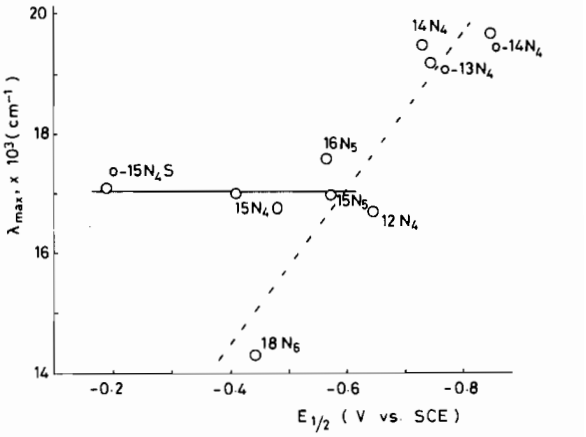

Fig. 4. Relationship between λ_{max} and $E_{1/2}$ for Cu(II) complexes of saturated macrocyclic ligands.

plex. Most positive $E_{1/2}$ values among macrocyclic polyamine–Cu(II) complexes can be seen for constrained octahedral $18N_6$–Cu(II) complex, which increases the stability of corresponding Cu(I) species. Thus, the positive shift of $E_{1/2}$ value *i.e.* the stability of Cu(I) species is in the order of octahedral > square-pyramidal > square-planar coordination geometry.

The 15-membered N_5, N_4O and N_4S macrocyclic ligand bind to Cu(II) by N, O and S atom at apical position with square-pyramidal geometry, respectively. The order of increasingly positive potential shift by fifth axial ligation is S > O > N atom. The specific Cu–S bond on apex stabilizes also the Cu(I) species, as discussed in following section.

Relationships between Redox Potentials and Spectroscopic Properties

In terms of the MO binding scheme as defined to the Cu(II) complex with $3d_{x^2-y^2}$ ground state [35], a positive hole occupying the $3d_{x^2-y^2}$ orbital with lowest energy level should be effectively stabilized by the in-plane ligand splitting Δ. Therefore, one can expect that a large ligand field splitting Δ results in a higher degree of negative shift in the observed $E_{1/2}$ value [36]. In fact, a linear relationship is being held between the λ_{max} and the $E_{1/2}$ values in the Cu(II) complexes of macrocyclic polyamines as illustrated by the dotted line in Fig. 4. We obtained the proportional correlation by the least squares method with a correlation coefficient $r^2 = 0.85$;

$$E_{1/2} = -7.67 \times 10^{-5} \times \lambda_{max} + 0.710 \quad (1)$$

On the other hand, the $3d_{x^2-y^2}$ ground state electronic configuration can be mixed with the electronic excited state due to the spin–orbital interaction (λ), thus g values can be expressed in terms of the ligand field splitting Δ [37];

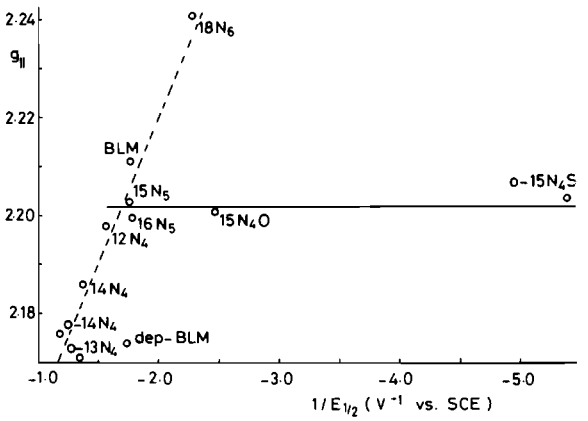

Fig. 5. Relationship between $g_{\parallel}$ and $1/E_{1/2}$ for Cu(II) complexes of saturated macrocyclic ligands, BLM and dep-BLM.

$$g_{\parallel} = 2.0023 \left(1 - \frac{4\alpha^2\lambda}{\Delta}\right) \quad (2)$$

$$g_{\perp} = 2.0023 \left(1 - \frac{\alpha^2\lambda}{\Delta}\right) \quad (3)$$

On replacing the relation (1) with (2), a linear relation should hold between the $g_{\parallel}$ components and the $1/E_{1/2}$ values. As illustrated in Fig. 5, a plot of $g_{\parallel}$ value *vs.* $1/E_{1/2}$ indeed shows the linear relation for the Cu(II) complexes, which contain only the N atoms as the donor set.

The plots for the Cu(II) complexes of $14N_4$, o-$14N_4$ and o-$13N_4$, grouping at the bottom of the dependence with the smaller $g_{\parallel}$ and the higher $1/E_{1/2}$, justify the fact that the Cu-N_4 arrangements of these complexes are in the square-planar geometry. The plots for Cu(II) complexes of $12N_4$, $15N_5$ and $16N_5$ locating in the middle suggest that the off-planar displacement of the Cu atoms from square basal plane, that is, an off-planar distortion to pyramidal geometry, should be taken into account in addition to the effect of apical ligation of the N atom, since the cavity size of N_4 basal plane is too small to accommodate Cu(II) ion in these complexes. The plot of $18N_6$–Cu(II) complex with the lowest $1/E_{1/2}$ value and $g_{\parallel}$ value should be attributed to the restricted coordination of Cu(II) ion in the constrained octahedral geometry. Of interest is that the value for BLM–Cu(II) complex noted in Fig. 5 is positioned in the vicinity of those for Cu(II) complexes of $15N_5$ and $16N_5$, but the value for dep-BLM–Cu(II) complex is markedly shifted to the region defined Cu(II) complexes of $14N_4$, o-$14N_4$ and o-$13N_4$ with square-planar structure.

From the linear dependence of $g_{\parallel}$ *vs.* $1/E_{1/2}$ observed values, some important features on the coordination geometry of BLM–Cu(II) complex can be assumed in comparison with the parameters of the macrocyclic polyamine–Cu(II) complexes. The Cu(II) ion in the BLM–Cu(II) complex is not situated on the square-planar group and the octahedral, but on the pyramidal as can be seen in Fig. 5. From both this and the X-ray analysis of the P-3A–Cu(II) complex [38] and that of $12N_4$ derivative ligands –Cu(II) complexes [39], a displacement (0.2–0.5 Å) of Cu(II) ion from the square basal plane would be probable in the metal chromophore of BLM–Cu(II) complex under the proposed coordination geometry [2, 26].

A significant effect of the primary amino group axially coordinated for the BLM–Cu(II) complex, is now evident from the plot. Removal of the ligation of primary amino group well documented for dep-BLM–Cu(II) complex, results in an effective increase in the in-plane ligand field, along with a modification of the ligand geometry in the Cu-N_4 square basal plane.

Of particular interest is the fact that the five coordinated square-pyramidal complexes with S, O and N axial donors give the plot on the parallel line close to the redox potential axis. Since the spectroscopic results show the small deviation from the ligand geometry in these complexes, the respective differences in the redox potentials will reflect the effectiveness of the apical donor to stabilize the Cu(I) complex. One can understand that these findings by the combination of electrochemical and spectroscopic methods well characterize the effects of the fifth axial N, O, and S donor atom in the square-pyramidal array.

The correlations indeed fit the stabilization of Cu(I) species. It has been known that the Cu(I) ion favors not only a distortion from the square-planar geometry, but also the π-acceptor (soft) ligand [40, 41]. The redox reaction for the o-$15N_4$-S–Cu(II) complex occurs easily by enhanced stabilization for Cu(I) species because of Cu(I) being a soft metal center. The axial O donor gives an intermediate effect between N and S donor. This tendency is consistent with the result for equatorial ligation, that is, $N_2S_2 > N_2O_2 > N_4$ donor sets [42].

A similar positive shift of $E_{1/2}$ value for the distorted square-pyramidal o-$15N_4$S–Cu(II) complex is well demonstrated for the glutathione–Cu(II) complex with fifth axial S donor [24]. The positive $E_{1/2}$ (+0.41 V *vs.* NHE) cited for galactose oxidase [43] is now documented in terms of the effect of axially coordinated S atoms, which has been already proposed by Kelly-Falcoz *et al.* [44]. In addition, the ESR parameters and its line shape for galactose oxidase [45] are close to those of violet glutathione–Cu(II) complex [3].

In conclusion, the plots of λ_{max} *vs.* $E_{1/2}$ and/or $g_{\parallel}$ *vs.* $1/E_{1/2}$ for the present Cu(II) complexes have linear correlations. $E_{1/2}$ values are very sensitive

to the variation of the ligation atom at apical position for five coordinated Cu(II) complexes. The combinations of electrochemical and spectroscopic features characterize the fifth axial donor of the square-pyramidal array.

The BLM–Cu(II) complex exhibits very similar characteristic properties to those of the $15N_5$–Cu(II) complex. The feature of axial S donor for the glutathione–Cu(II) complex was also documented by the electrochemical and spectroscopic properties of the o-$15N_4S$–Cu(II) complex. A similar behavior is expected to be applicable to the case of other copper–peptide systems.

Acknowledgements

The authors thank Drs. M. Kishita and W. Mori of College of General Education, Osaka University for MCD measurement, Miss J. Hirai of Faculty of Science, Ehime University for assitance, Dr. Y. Sugiura of Faculty of Pharmaceutical Sciences, Kyoto University and Dr. T. Takita of Institute of Microbial Chemistry for kind advice. This study was supported in part by a grant from the Ministry of Education, Science, and Culture.

References

1 J. J. Christensen, D. J. Eatough and R. M. Izatt, *Chem. Rev., 74,* 351 (1974).
2 Y. Sugiura, K. Ishizu and K. Miyoshi, *J. Antibiotics, 32,* 453 (1979).
3 K. Miyoshi, Y. Sugiura, K. Ishizu, Y. Iitaka and H. Nakamura, *J. Am. Chem. Soc., 102,* 6130 (1980).
4 Y. Sugiura, *J. Am. Chem. Soc., 102,* 5208 (1980).
5 M. Goldberg, S. Vuk-Pavlović and I. Pecht, *Biochemistry, 19,* 5181 (1980).
6 T. Sakurai, S. Suzuki and A. Nakahara, *Bull. Chem. Soc. Jpn, 54,* 2313 (1981).
7 F. V. Lovecchio, E. S. Gore and D. H. Busch, *J. Am. Chem. Soc., 96,* 3109 (1974).
8 A. Bencini, L. Fabbrizzi and A. Poggi, *Inorg. Chem., 20,* 2544 (1981).
9 A. G. Lappin, C. K. Murray and D. W. Margerum, *Inorg. Chem., 17,* 1630 (1978).
10 Y. Sugiura and Y. Mino, *Inorg. Chem., 18,* 1336 (1979).
11 M. C. Styka, R. C. Smierciak, E. L. Blinn, R. E. Desimone and J. V. Passariello, *Inorg. Chem., 17,* 82 (1978).
12 M. Kodama and E. Kimura, *J. Chem. Soc. Dalton,* 1976, 116;
M. Kodama and E. Kimura, *J. Chem. Soc. Dalton,* 1976, 1720;
M. Kodama and E. Kimura, *J. Chem. Soc. Dalton,* 1976, 2341;
M. Kodama and E. Kimura, *J. Chem. Soc. Dalton,* 1977, 1473.
13 I. Tabushi, H. Okino and Y. Kuroda, *Tetrahedron Letters, 48,* 4439 (1976).
14 M. Kodama and E. Kimura, *J. Chem. Soc. Dalton,* 1979, 325;
M. Kodama and E. Kimura, *J. Chem. Soc. Dalton,* 1978, 104;
M. Kodama, E. Kimura and S. Yamaguchi, *J. Chem. Soc. Dalton,* 1980, 2536.
15 J. J. Bour, P. J. M. W. L. Birker and J. J. Steggerda, *Inorg. Chem., 10,* 1202 (1971).
16 D. P. Rillema, J. F. Endicott and E. Papaconstantinou, *Inorg. Chem., 10,* 1739 (1971).
17 R. S. Nickolson and I. Shain, *Anal. Chem., 36,* 706 (1964).
18 M. Kodama and E. Kimura, *J. Chem. Soc. Dalton,* 1978, 1081.
19 L. Fabbrizzi, M. Micheloni and P. Paoletti, *J. Chem. Soc. Chem. Comm.,* 1978, 833.
20 J. Bjerrum, C. J. Ballhausen and C. K. Jorgenson, *Acta Chem. Scand., 8,* 1275 (1954).
21 B. J. Hathaway and D. E. Billing, *Coord. Chem. Rev., 5,* 143 (1970).
22 P. Kroneck, *J. Am. Chem. Soc., 97,* 3839 (1975).
23 K. Ishizu, S. Murata, K. Miyoshi, Y. Sugiura, T. Takita and H. Umezawa, *J. Antibiotics, 34,* 994 (1981).
24 K. Miyoshi, Y. Sugiura, H. Tanaka and K. Ishizu, to be published.
25 L. Fabbrizzi, P. Paoletti and A. B. P. Lever, *Inorg. Chem., 15,* 1502 (1976).
26 T. Takita, Y. Muraoka, T. Nakatani, A. Fujii, Y. Iitaka and H. Umezawa, *J. Antibiotics, 31,* 1073 (1978).
27 K. Ishizu, T. Haruta, Y. Kohno, K. Mukai, K. Miyoshi and Y. Sugiura, *Bull. Chem. Soc. Jpn., 53,* 3513 (1980).
28 A. S. Brill, 'Molecular Biology Biochemistry and Biophysics. 26. Transition Metals in Biochemistry', Ed. A. Kleinzeller, Springer-Verlag, New York, 1977, p. 43.
29 A. F. Garito and B. B. Wagland, *J. Am. Chem. Soc., 91,* 866 (1969).
30 Y. Sugiura, *Inorg. Chem., 17,* 2176 (1978).
31 I. Bertini, D. Gatteschi and A. Scozzafava, *Inorg. Chem., 16,* 1973 (1977).
32 B. Hathaway, M. Duggan, A. Murphy, J. Mullane, C. Power, A. Walsh and B. Walsh, *Coord. Chem. Rev., 36,* 267 (1981).
33 J. M. Palmer, E. Papaconstantinou and J. F. Endicott, *Inorg. Chem., 8,* 1516 (1969).
34 D. C. Olson and J. Vasilevskis, *Inorg. Chem., 10,* 463 (1971).
35 A. Abraham and B. Bleany, 'Electron Paramagnetic Resonance of Transition Ions', Clarendon Press, Oxford, 1970, p. 365.
36 F. P. Bossu, K. L. Chellappa and D. W. Margerum. *J. Am Chem. Soc., 99,* 2195 (1979).
37 T. Vängärd, 'Biological Applications of Electron Spin Resonance', Ed. J. R. Bolton, Wiley–Interscience, New York, 1972, p. 411.
38 Y. Iitaka, H. Nakamura, T. Nakatani, Y. Muraoka, A. Fujii, T. Takita and H. Umezawa, *J. Antibiotics, 31,* 1070 (1978).
39 T.Sakurai, K. Kobayashi, A. Hasegawa, S. Tsuboyama and K. Tsuboyama, *Acta Cryst., B38,* 107 (1982).
40 V. Miskowski, S. P. W. Tang, T. G. Spiro, E. Shapiro and T. H. Moss, *Biochemistry, 14,* 1244 (1975).
41 H. Yokoi and A. W. Addison, *Inorg. Chem., 16,* 1341 (1977).
42 G. S. Patterson and R. H. Holm, *Bioinorg. Chem., 4,* 257 (1975).
43 G. A. Hamilton, P. K. Adolf, J. de Jersey, G. C. DuBois, G. R. Drykacy and R. D. Libby, *J. Am. Chem. Soc., 100,* 1899 (1978).
44 F. Kelly-Falcoz, H. Greenberg and B. L. Horecker, *J. Biol. Chem., 240,* 2966 (1965);
L. Cleveland, R. E. Coffman, P. Coon and L. Davis, *Biochemistry, 14,* 1108 (1975).
45 R. S. Giordano and R. D. Bereman, *J. Am. Chem. Soc., 96,* 1019 (1974).